

Supporting Information

Macrocyclic $\text{Se}_4\text{N}_2[7,7]$ Ferrocenophane and $\text{Se}_2\text{N}[10]$ ferrocenophane Containing Benzyl Unit: Synthesis, Complexation, Crystal Structures, Electrochemical and Optical Properties

Jian Qu,^{a,b} Yinglin Song,^c Wei Ji,^{a,d} Su Jing,^{*a} Dun-Ru Zhu,^{*d} Wei Huang^{*b},
Mengxi Zheng^e, Yanle Li^e, Jing Ma^e

^aSchool of Chemistry and Molecular Engineering, Nanjing Tech University, Nanjing 211800, China.

^bInstitute of Advanced Materials, Nanjing Tech University, Nanjing 210009, China.

^cCollege of Physics, Optoelectronics and Energy, Soochow University, Suzhou 215006, China

^dSchool of Chemical Engineering, Nanjing Tech University, Nanjing 210009, China.

^eInstitute of Theoretical and Computational Chemistry, School of Chemistry and Chemical Engineering, Nanjing University, Nanjing 210093, China

Table of contents

Table S1 Selected bond lengths (Å) and bond angles (°) for **L1-L2**

Table S2 Selected bond lengths (Å) and bond angles (°) for **1-5**

Figure S1 The C-H... π interactions involving intermolecular C2-H2A...Cg (C1-C5) of **L1**.

Figure S2 The C-H... π interactions involving intermolecular C12-H12A...Cg of **L2**.

Figure S3 Changes in the absorption spectra of receptor **L1** (2×10^{-5} M) with increasing concentration of Hg^{2+} (0 to 4.0 equiv.) in a CH_3CN solution.

Figure S4 Changes in the absorption spectra of receptor **L2** (2×10^{-5} M) with increasing concentration of Cu^{2+} (0 to 3.0 equiv.) in a CH_3CN solution (inset: Cu^{2+} titration profile at 295 nm).

Figure S5 (a) Absorbance of **L1** at different concentrations of Cu^{2+} added, normalized between the minimum absorbance and the maximum absorbance intensity. The detection limit was determined to be 1.03×10^{-5} M. (b) Absorbance of **L2** at different concentrations of Cu^{2+} added, normalized between the minimum absorbance and the maximum absorbance intensity. The detection limit was determined to be 8.64×10^{-6} M.

Figure S6 The association constant for **L2**.

Figure S7 The open aperture and closed aperture Z-scan results at 532 nm for **L1** in CH_3CN .

Figure S8 Cyclic voltammogram of **L1** (black line) in acetonitrile upon addition of Cu^{2+} (red line) and Hg^{2+} (blue line).

Figure S9 Cyclic voltammogram of **L2** (black line) in acetonitrile upon addition of Cu^{2+} (red line) and Hg^{2+} (blue line).

Figure S10 UV-vis spectra of **L1** and 1,5,9,13-tetraselena[16]-naphtho[1,8-*c,d*]-ferrocenophane.

Figure S11 The frontier orbitals of **3** and **L1**

Table S1 Selected bond lengths (Å) and bond angles (°) for **L1-L2**^a

L1				L2			
Se1-C1	1.911(2)	Se1-C11 ⁱ	1.954(3)	Se1-C1	1.901(4)	N1-C12	1.471(5)
Se2-C6	1.902(3)	Se2-C13	1.960(2)	Se1-C11	1.964(4)	N1-C13	1.474(5)
N1-C12	1.463(3)	N1-C14	1.472(3)	Se2-C6	1.906(4)	N1-C15	1.461(5)
N1-C15	1.461(3)			Se2-C14	1.944(4)		
C1-Se1-C11 ⁱ	98.52(10)	C12-N1-C14	112.4(2)	C1-Se1-C11	99.43(16)	C6-Se2-C14	102.93(16)
C6-Se2-C13	99.85(11)	C12-N1-C15	111.2(2)	C12-N1-C15	110.6(3)	C13-N1-C15	110.5(3)
C14-N1-C15	112.50(19)			C12-N1-C13	111.4(3)		

^a Symmetry code i: -x, y, 0.5-z.

Table S2 Selected bond lengths (Å) and bond angles (°) for **1-5^a**

1		2		3		4		5	
Br1-Cu1	2.3594(15)	I1-Cu1	2.5146(8)	N2-Cu1	1.953(5)	O5-Cu1	2.077(3)	Cl1-Pd1	2.2741(16)
Se1-Cu1	2.4054(14)	Se1-Cu1	2.4815(9)	Se1-Cu1	2.4025(19)	Se1-Cu1	2.3623(6)	Se2-Pd1	2.4297(9)
Se1-C1	1.886(8)	Se1-C1	1.906(5)	Se1-C1	1.902(5)	Se1-C1	1.898(3)	Se1-C1	1.895(6)
Se1-C11	1.955(8)	Se1-C11	1.974(6)	Se1-C11	1.969(5)	Se1-C11	1.962(3)	Se1-C14	1.986(6)
Se2-Cu1	2.4364(16)	Se2-Cu1	2.4156(9)	Se2-Cu1	2.4306(18)	Se2-Cu1	2.4095(6)	Se1-Pd1	2.4198(9)
Se2-C9	1.894(8)	Se2-C6	1.908(5)	Se2-C6	1.908(6)	Se2-C6	1.907(3)	Se2-C6	1.871(7)
Se2-C14	1.958(9)	Se2-C14	1.971(5)	Se2-C14	1.983(5)	Se2-C14	1.974(4)	Se2-C11	1.983(6)
Cu1-N1	2.237(6)	Cu1-N1	2.232(4)	Cu1-N1	2.185(4)	Cu1-N1	2.184(3)	Pd1-N1	2.087(4)
N1-C15	1.503(10)	N1-C15	1.497(6)	N1-C15	1.488(7)	N1-C15	1.496(4)	N1-C15	1.543(8)
N1-C12	1.488(11)	N1-C12	1.473(6)	N1-C12	1.470(6)	N1-C12	1.483(4)	N1-C12	1.498(8)
N1-C13	1.476(10)	N1-C13	1.479(6)	N1-C13	1.485(7)	N1-C13	1.488(4)	N1-C13	1.513(7)
Cu1-Se1-C1	106.7(2)	Cu1-Se1-C1	112.14(17)	Cu1-Se1-C1	104.96(16)	Cu1-Se1-C1	107.55(11)	Pd1-Se1-C1	103.18(18)
Cu1-Se1-C11	91.5(2)	Cu1-Se1-C11	89.89(16)	Cu1-Se1-C11	90.15(16)	Cu1-Se1-C11	89.67(10)	Pd1-Se1-C14	94.06(18)
C1-Se1-C11	97.4(4)	C1-Se1-C11	97.0(2)	C1-Se1-C11	95.8(2)	C1-Se1-C11	98.95(15)	C1-Se1-C14	96.7(3)
Cu1-Se2-C9	110.6(2)	Cu1-Se2-C6	110.14(17)	Cu1-Se2-C6	109.75(18)	Cu1-Se2-C6	106.94(10)	Pd1-Se2-C6	108.65(19)
Cu1-Se2-C14	92.2(3)	Cu1-Se2-C14	91.54(17)	Cu1-Se2-C14	91.46(18)	Cu1-Se2-C14	90.22(11)	Pd1-Se2-C11	93.85(19)
Br1-Cu1-Se1	120.54(5)	I1-Cu1-Se1	110.10(3)	N2-Cu1-Se1	119.63(15)	O5-Cu1-Se1	122.73(9)	Cl1-Pd1-Se1	90.86(5)
Br1-Cu1-Se2	111.37(5)	I1-Cu1-Se2	125.51(3)	N2-Cu1-Se2	105.99(16)	O5-Cu1-Se2	105.59(9)	Cl1-Pd1-Se2	92.92(5)
Br1-Cu1-N1	114.74(17)	I1-Cu1-N1	115.94(10)	N2-Cu1-N1	116.06(19)	O5-Cu1-N1	106.76(12)	Cl1-Pd1-N1	177.76(14)
Se1-Cu1-Se2	122.64(5)	Se1-Cu1-Se2	117.32(3)	Se1-Cu1-Se2	128.14(4)	Se1-Cu1-Se2	127.52(2)	Se1-Pd1-Se2	176.20(3)
Se1-Cu1-N1	90.39(18)	Se1-Cu1-N1	89.47(11)	Se1-Cu1-N1	90.92(12)	Se1-Cu1-N1	92.64(7)	Se1-Pd1-N1	88.64(14)
Se2-Cu1-N1	88.93(17)	Se2-Cu1-N1	90.39(11)	Se2-Cu1-N1	90.12(13)	Se2-Cu1-N1	91.87(7)	Se2-Pd1-N1	87.57(13)

Cu1-N1-C12	107.1(5)	Cu1-N1-C12	106.8(3)	Cu1-N1-C12	108.5(3)	Cu1-N1-C12	107.7(2)	Pd1-N1-C12	107.8(3)
Cu1-N1-C13	109.3(5)	Cu1-N1-C13	106.1(3)	Cu1-N1-C13	108.6(3)	Cu1-N1-C13	106.5(2)	Pd1-N1-C13	109.9(3)
Cu1-N1-C15	107.5(4)	Cu1-N1-C15	110.6(3)	Cu1-N1-C15	106.5(3)	Cu1-N1-C15	108.66(19)	Pd1-N1-C15	108.5(3)
C12-N1-C13	109.8(6)	C12-N1-C13	110.9(4)	C12-N1-C13	109.6(4)	C12-N1-C13	110.5(3)	C12-N1-C13	108.0(5)
C12-N1-C15	110.9(7)	C12-N1-C15	111.9(4)	C12-N1-C15	110.8(4)	C12-N1-C15	110.9(3)	C12-N1-C15	112.9(5)
C13-N1-C15	112.1(6)	C13-N1-C15	110.3(4)	C13-N1-C15	112.7(4)	C13-N1-C15	112.5(3)	C13-N1-C15	109.8(5)

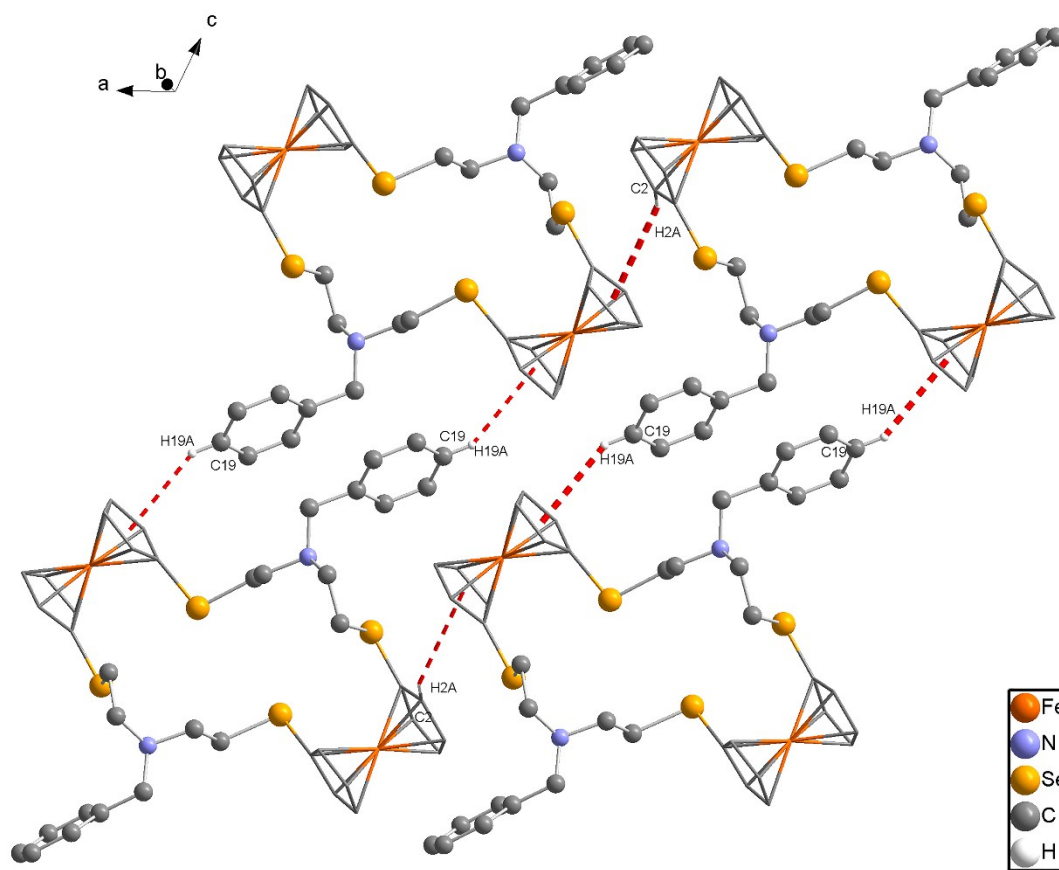


Figure S1 The C-H... π interactions involving intermolecular C2-H2A...Cg (C1-C5) of L1.

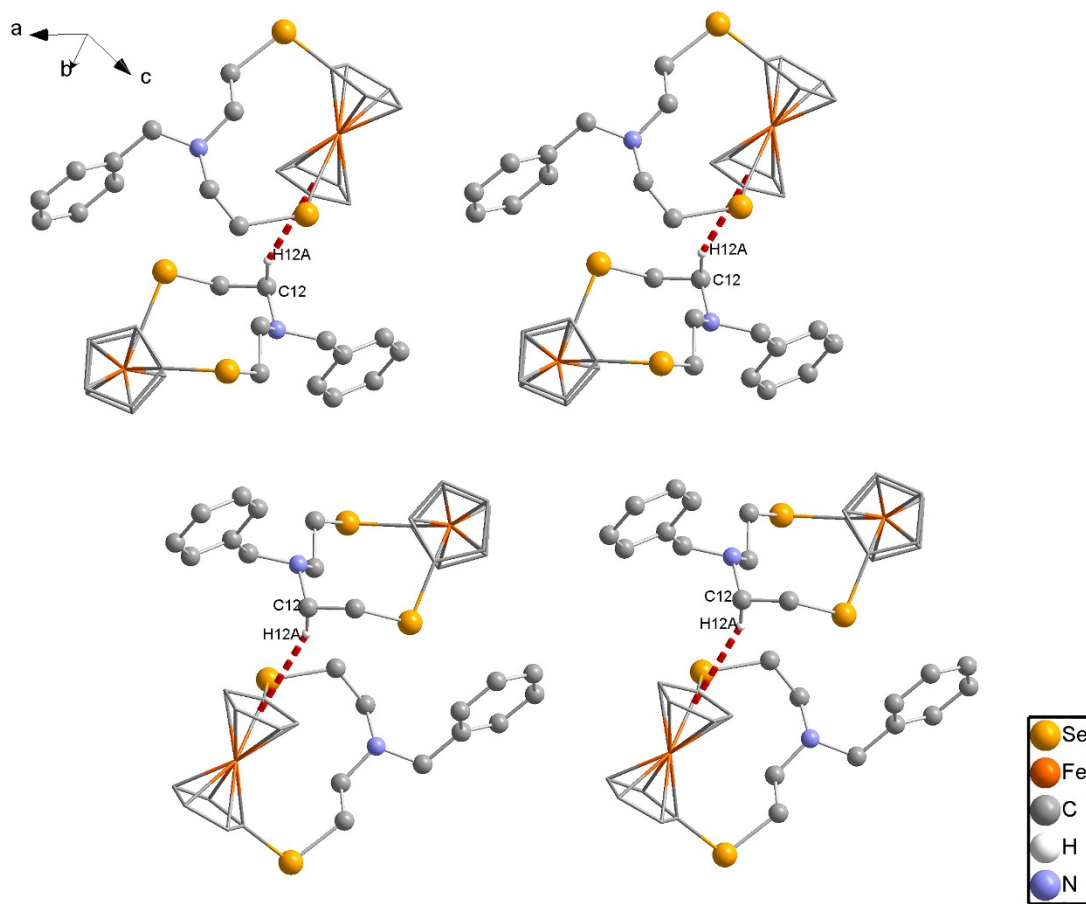


Figure S2 The C-H... π interactions involving intermolecular C12-H12A...Cg of L2.

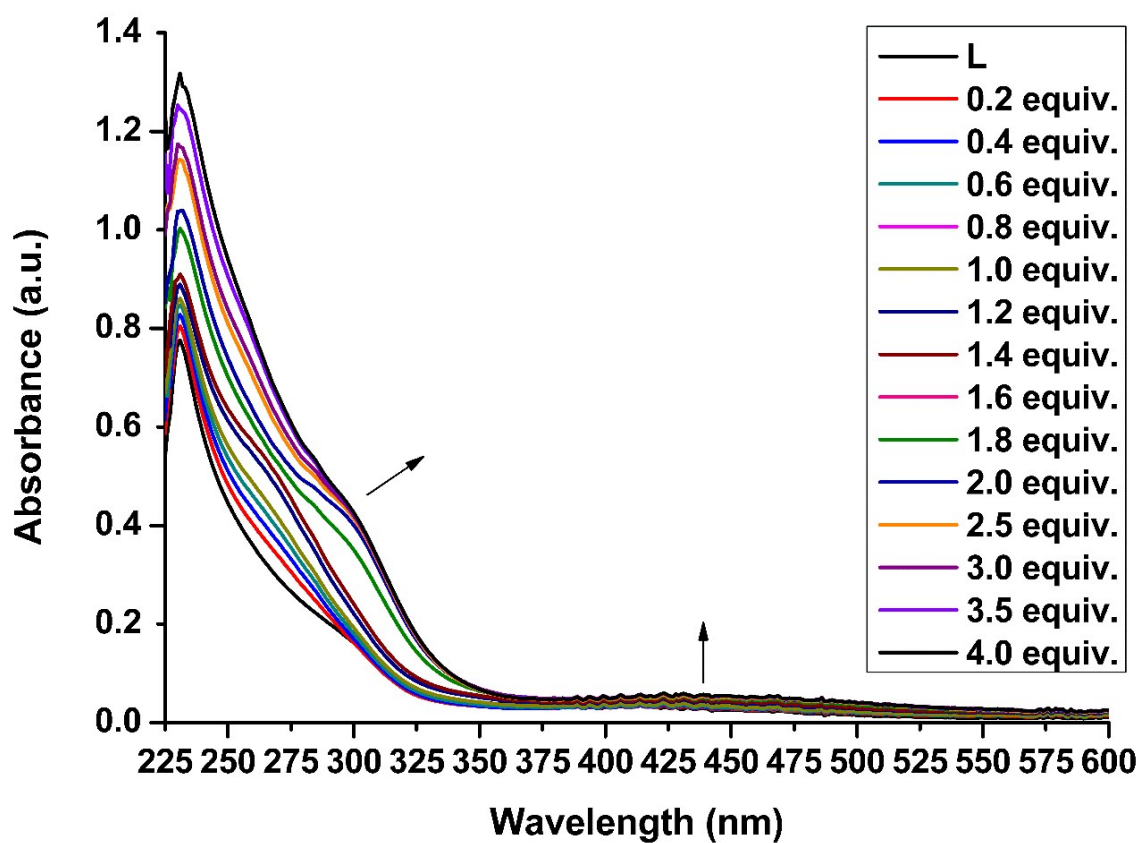


Figure S3 Changes in the absorption spectra of receptor **L1** (2×10^{-5} M) with increasing concentration of Hg^{2+} (0 to 4.0 equiv.) in a CH_3CN solution.

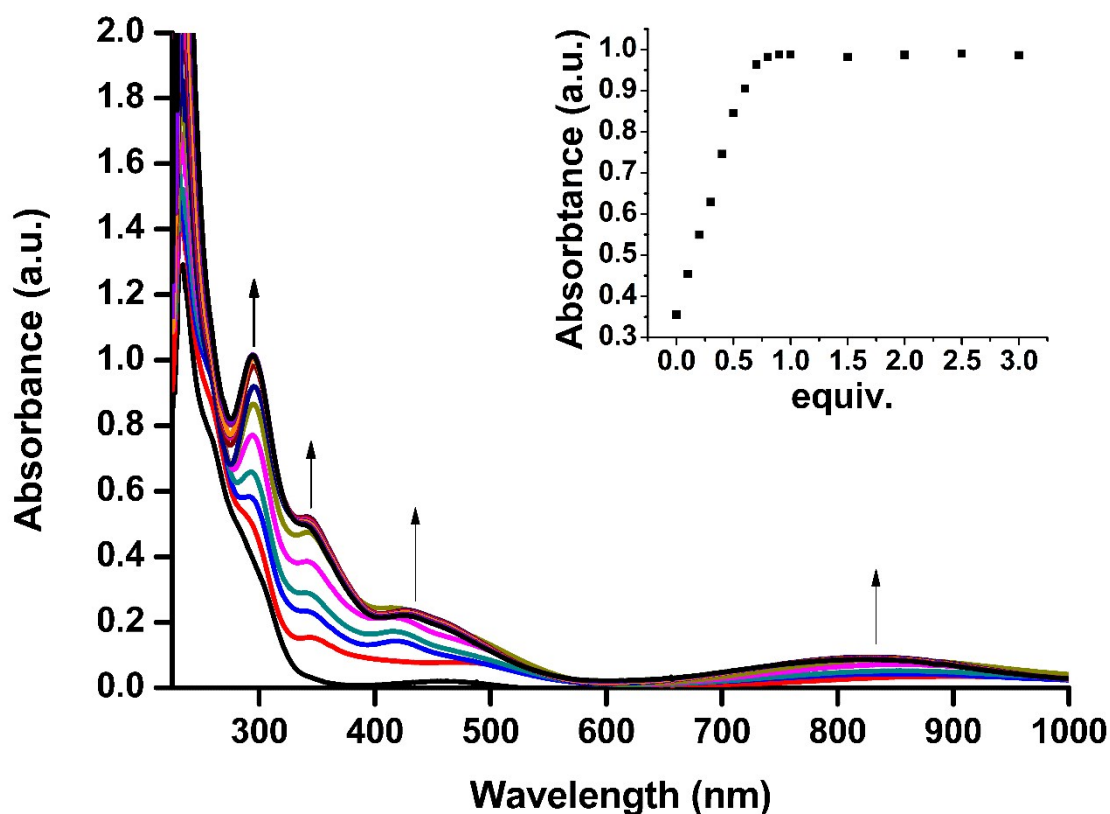


Figure S4 Changes in the absorption spectra of receptor **L2** (2×10^{-5} M) with increasing concentration of Cu^{2+} (0 to 3.0 equiv.) in a CH_3CN solution (inset: Cu^{2+} titration profile at 295 nm).

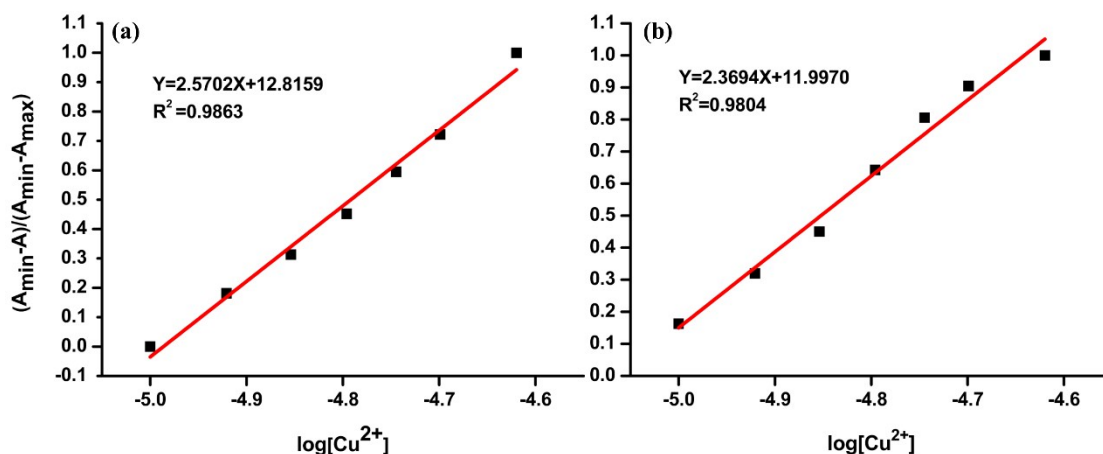


Figure S5 (a) Absorbance of **L1** at different concentrations of Cu^{2+} added, normalized between the minimum absorbance and the maximum absorbance intensity. The detection limit was determined to be 1.03×10^{-5} M. (b) Absorbance of **L2** at different concentrations of Cu^{2+} added, normalized between the minimum absorbance and the maximum absorbance intensity. The detection limit was determined to be 8.64×10^{-6} M.

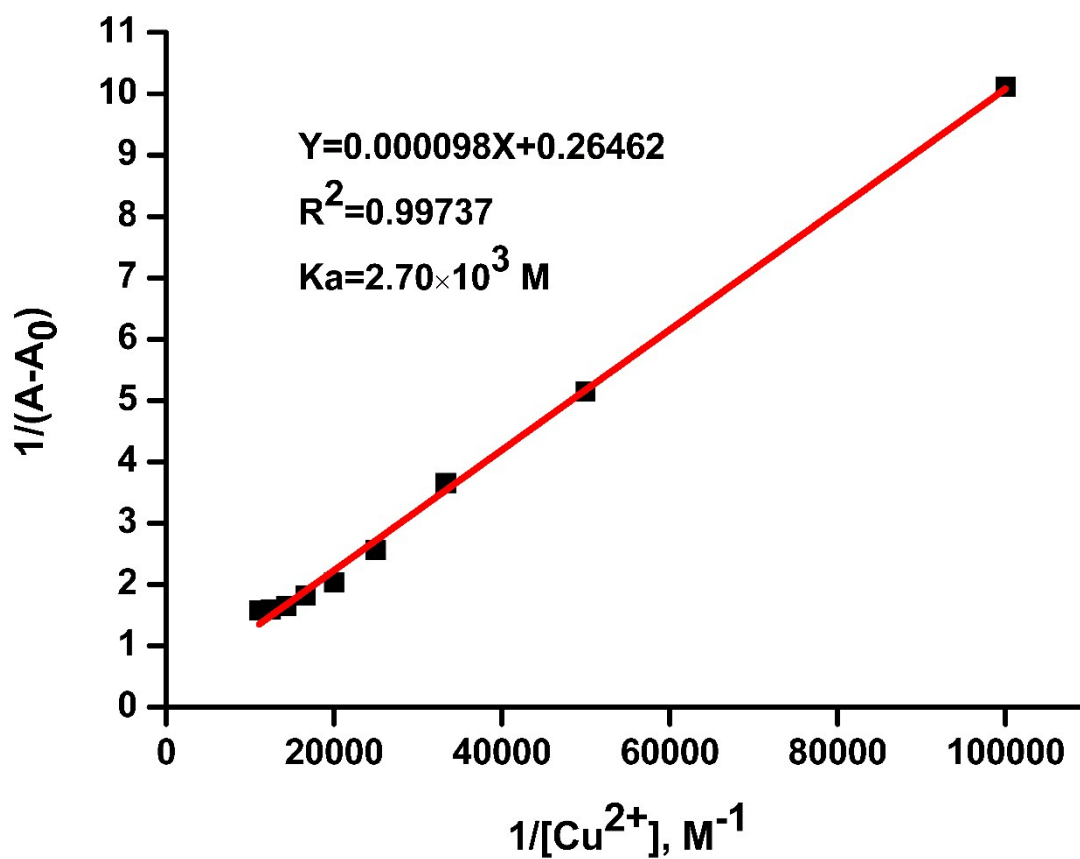


Figure S6 The association constant for L2.

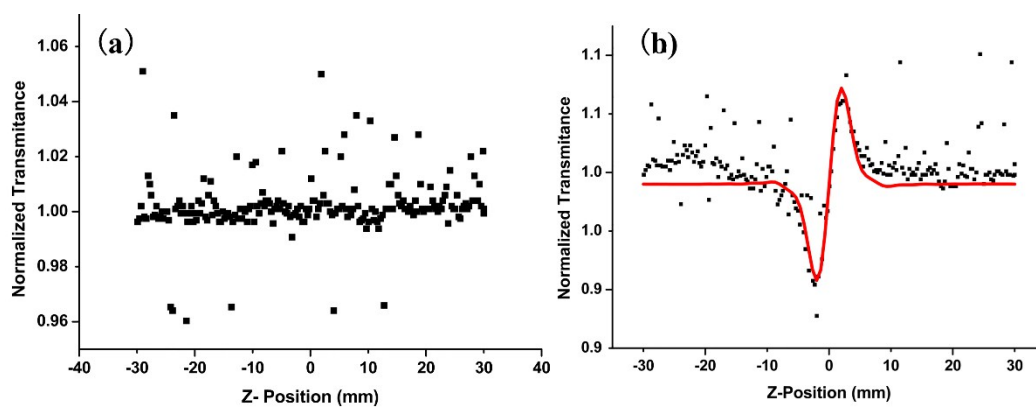


Figure S7 The open aperture and closed aperture Z-scan results at 532 nm for L1 in CH₃CN

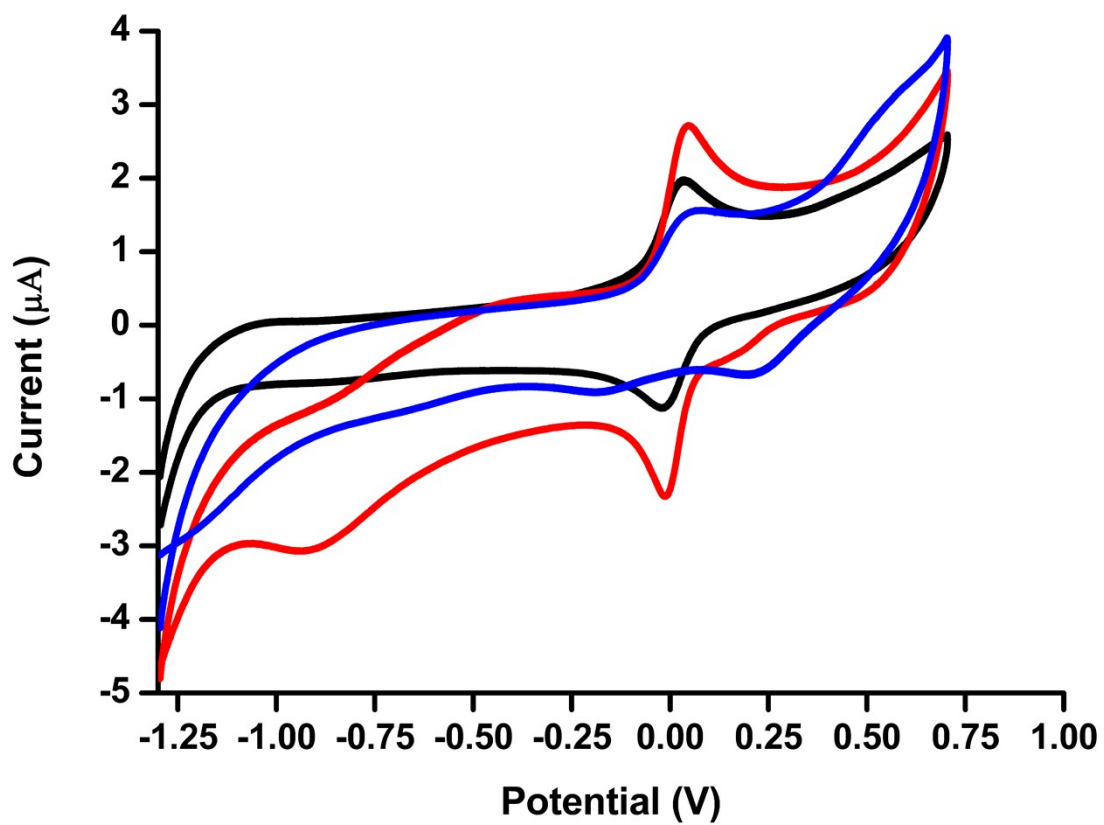


Figure S8 Cyclic voltammogram of L1 (black line) in acetonitrile upon addition of Cu^{2+} (red line) and Hg^{2+} (blue line).

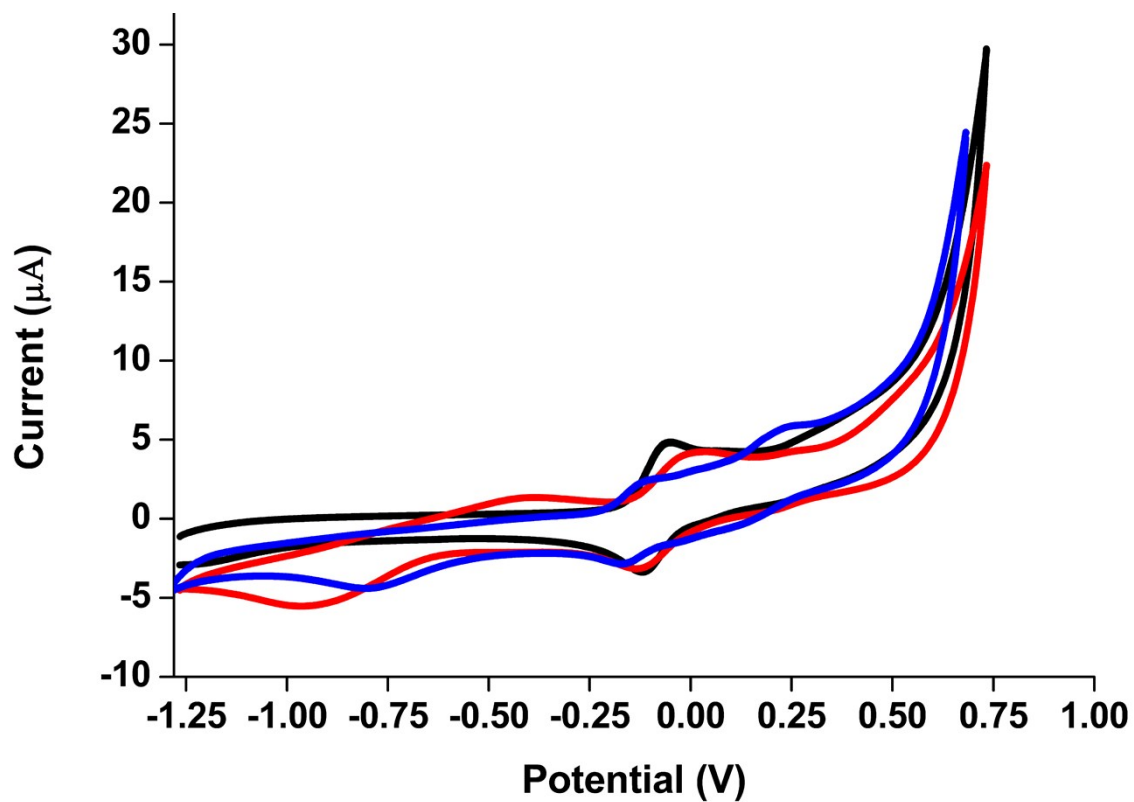


Figure S9 Cyclic voltammogram of L2 (black line) in acetonitrile upon addition of Cu^{2+} (red line) and Hg^{2+} (blue line).

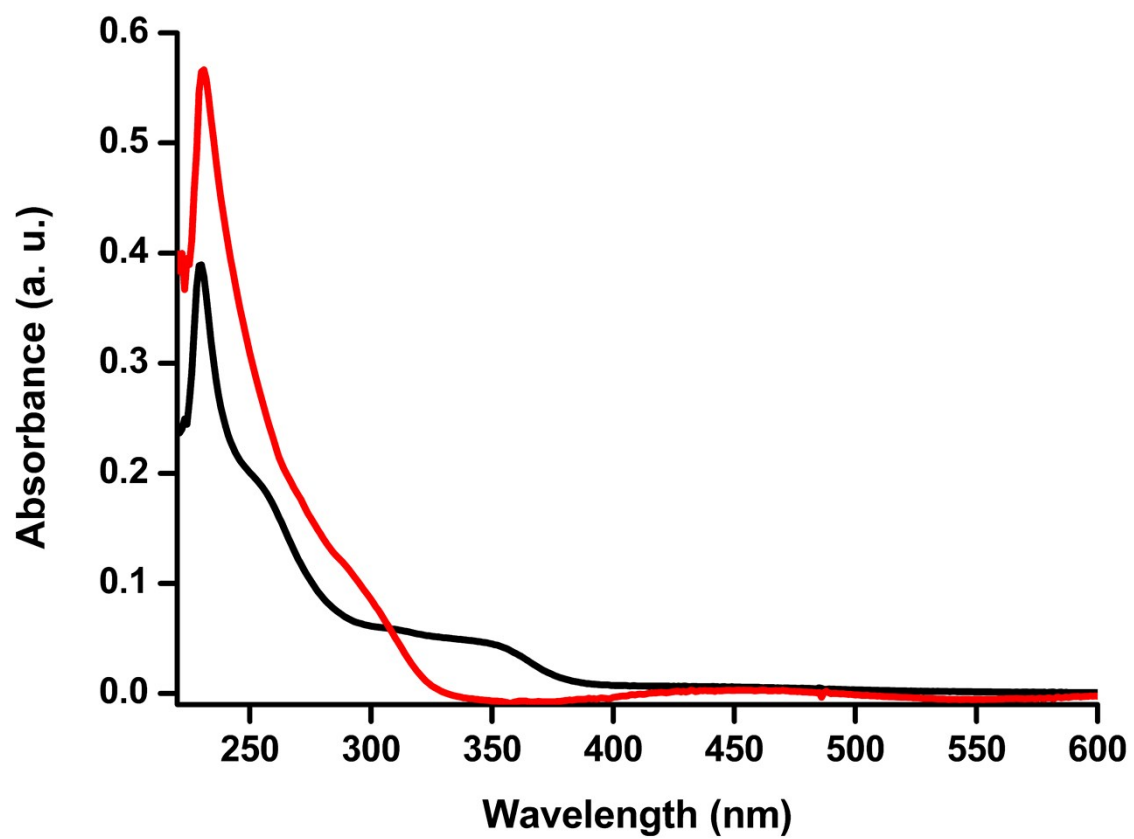
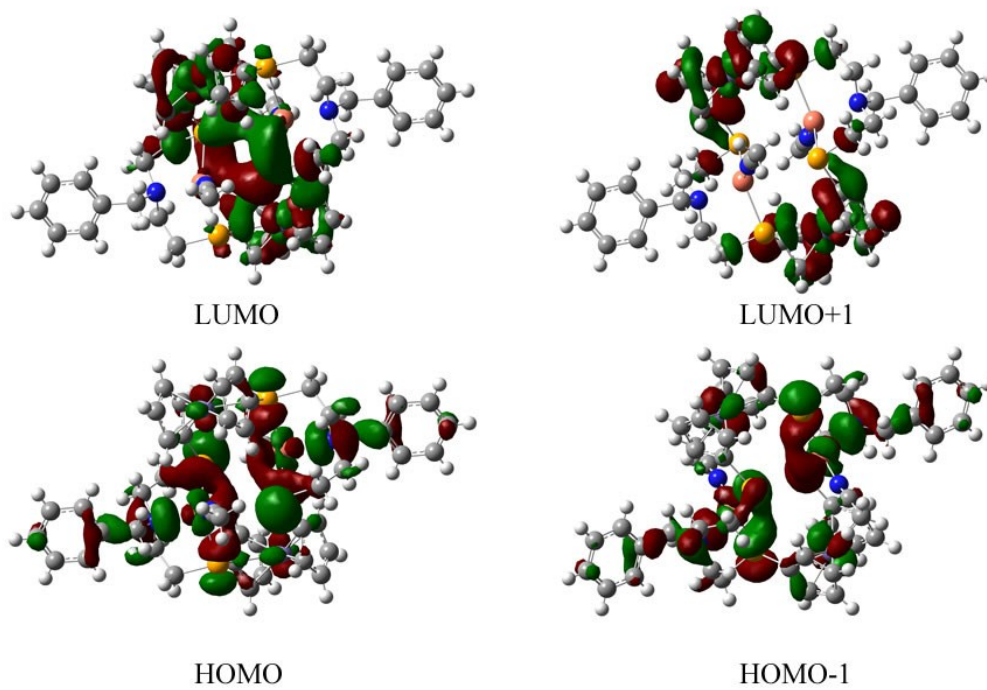


Figure S10 UV-vis spectra of **L1** (red line) and 1,5,9,13-tetraselena[16]-naphtho[1,8-*c,d*]-ferrocenophane (black line)

(a) Frontier Orbitals of **3**



(a) Frontier Orbitals of **L1**

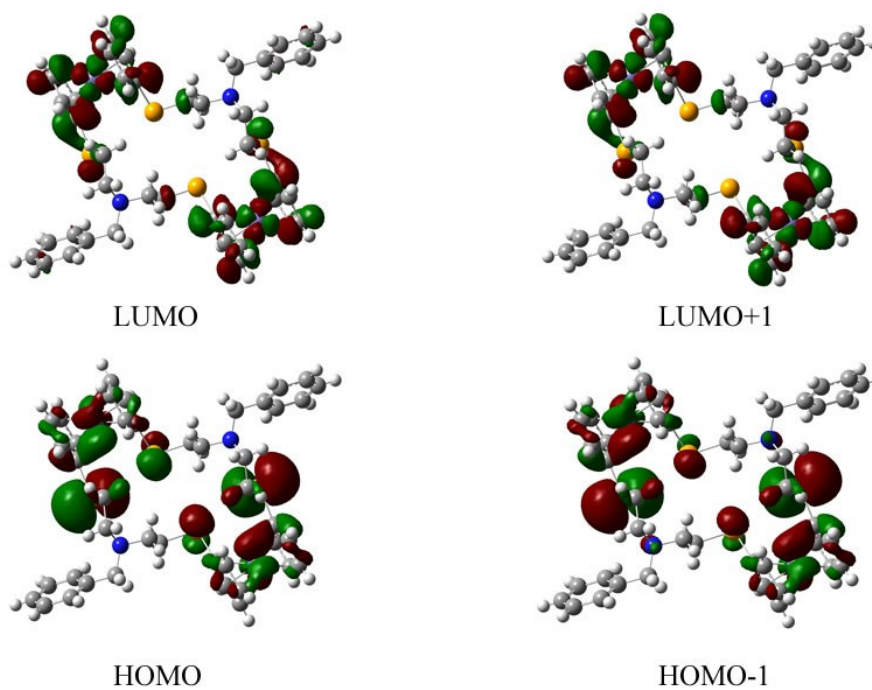


Figure S11 The frontier orbitals of **3** and **L1**